Biochemical and Biophysical Research Communications 437 (2013) 426–432

Contents lists available at SciVerse ScienceDirect

Biochemical and Biophysical Research Communications

journal homepage: www.elsevier.com/locate/ybbrc

Copper deficiency alters cell bioenergetics and induces mitochondrial fusion through up-regulation of MFN2 and OPA1 in erythropoietic cells

Rodrigo I. Bustos [a], Erik L. Jensen [a], Lina M. Ruiz [a], Salvador Rivera [a], Sebastián Ruiz [a], Felipe Simon [a,b], Claudia Riedel [a,b], David Ferrick [c], Alvaro A. Elorza [a,b,*]

[a] Center for Biomedical Research, Faculty of Biological Sciences and Faculty of Medicine, Universidad Andres Bello, Santiago, Chile
[b] Millennium Institute of Immunology and Immunotherapy, Santiago, Chile
[c] Seahorse Bioscience, Billerica, MA, USA

ARTICLE INFO

Article history:
Received 21 June 2013
Available online 4 July 2013

Keywords:
Mitochondria
Bioenergetics
Copper
Glycolysis
MFN2
OPA1
Mitochondrial dynamics

ABSTRACT

Copper is essential in cell physiology, participating in numerous enzyme reactions. In mitochondria, copper is a cofactor for respiratory complex IV, the cytochrome c oxidase. Low copper content is associated with anemia and the appearance of enlarged mitochondria in erythropoietic cells. These findings suggest a connection between copper metabolism and bioenergetics, mitochondrial dynamics and erythropoiesis, which has not been explored so far. Here, we describe that bathocuproine disulfonate-induced copper deficiency does not alter erythropoietic cell proliferation nor induce apoptosis. However it does impair erythroid differentiation, which is associated with a metabolic switch between the two main energy-generating pathways. That is, from mitochondrial function to glycolysis. Switching off mitochondria implies a reduction in oxygen consumption and ROS generation along with an increase in mitochondrial membrane potential. Mitochondrial fusion proteins MFN2 and OPA1 were up-regulated along with the ability of mitochondria to fuse. Morphometric analysis of mitochondria did not show changes in total mitochondrial biomass but rather bigger mitochondria because of increased fusion. Similar results were also obtained with human CD34+, which were induced to differentiate into red blood cells. In all, we have shown that adequate copper levels are important for maintaining proper mitochondrial function and for erythroid differentiation where the energy metabolic switch plus the up-regulation of fusion proteins define an adaptive response to copper deprivation to keep cells alive.

1. Introduction

Copper is an essential transition metal that acts as a cofactor in many enzymes, playing key roles in cell metabolism and bioenergetics. Copper is an integral part of the cytochrome c oxidase, the complex IV (CIV) of the respiratory chain, and it is needed for its assembly and function [1,2]. Hallmarks of dysfunctional copper metabolism are the Wilson's and Menkes diseases that are inherited disorders [1–3].

Acquired copper deficiency has also been reported and can be induced by a poor copper and/or high zinc diet as well as conditions like gastric surgery, parenteral nutrition and tube feeding [4–6]. Clinical manifestations of acquired copper deficiency are anemia, bone marrow dysplasia, neutropenia and neuromyelopathy [7–10]. Interestingly, the appearance of enlarged mitochondria was described in early precursors of bone marrow, in hepatocytes and myocardium in humans and rats when under copper deficiency [11–14]. All these findings are suggesting a connection between copper content and bioenergetics, erythropoiesis and mitochondrial dynamics that has not been explored yet.

Erythropoiesis is highly dependent of mitochondrial metabolism because mitochondria are vital in processes such as energy production, heme biosynthesis and iron and copper metabolism [1,15,16]. As a byproduct, a considerable amount of ROS is generated by the respiratory chain itself and by the Fenton and-Haber-Weiss reactions. Mitochondria are extremely dynamic organelles, undergoing frequent fusion and fission events, the so-called mitochondrial dynamics (MtDy), which regulate their morphology, number and function. In erythropoiesis, there is an initial increase in mitochondrial number and biomass to accomplish heme biosynthesis and energy demands, followed by mitophagy at final stages of maturation [17,18]. Mitochondrial fusion is dependent on mitochondrial membrane potential (mt$\Delta\Psi$), GTP, the proteins mitofusin 1 and 2 (MFN1 and MFN2) and optic

* Corresponding author at: Universidad Andres Bello, Department of Biological Sciences, Faculty of Biological Sciences, Santiago, Chile.
E-mail address: aelorza@unab.cl (A.A. Elorza).

0006-291X/$ - see front matter © 2013 Elsevier Inc. All rights reserved.
http://dx.doi.org/10.1016/j.bbrc.2013.06.095

atrophy 1 (OPA1) in mammals [19]. Proteins involved in fission are DRP1/DNM1 (dynamin-related protein 1/dynamin 1) and FIS1 (Fission 1 homolog protein) [20,21].

Given that copper is part of CIV and its depletion stimulates the formation of enlarged mitochondria and induces anemia, we aim to explore if mitochondrial dynamics alterations are involved in this phenomenon as well as the bioenergetics of the two energy metabolic pathways, the oxidative phosphorylation and glycolysis, in erythropoietic cells.

2. Materials and methods

2.1. Reagents

Most antibodies were from Abcam. MitoTracker Green (MTG), MitoTracker Red CMXRos (MTR), tetramethylrhodamine methyl ester (TMRE) and dihydroethidium (DHE) were from Invitrogen. Polyethyleneglycol 1500 (PEG) was from Roche. Bathocuproine disulfonate (BCS), rotenone, carbonyl cyanide 4-(trifluoromethoxy)phenylhydrazone (FCCP), oligomycin, butyric acid, 3,3′,5,5′-tetramethylbenzidine were from Sigma–Aldrich.

2.2. Cell culture

K562 cells (ATCC) were maintained in RPMI 1640 medium (Hyclone), supplemented with 10% FBS (Hyclone), penicillin–streptomycin (Invitrogen) and GlutaMAX (Invitrogen). Differentiation was induced with 0.9 mM butyric acid. Cells expressing hemoglobin were quantitated with benzidine staining.

Human CD34+ cells were isolated using MACS® CD34 Microbead kit (Miltenyi Biotec) from umbilical cord blood and cultured as published [22] in Iscove's media supplemented with 30% FBS, penicillin–streptomycin, GlutaMAX, 120 μg/mL human holotransferrin (Biological Industries), 3 U/mL EPO (Proscan), 100 ng/mL SCF (Miltenyi Biotec) and 10 ng/mL IL-3 (Miltenyi Biotec).

2.3. Copper chelation

K562 cells were copper-deprived for 72 h in the presence of 10–30 μM BCS. CD34+ cells were cultured for 3 days after isolation to allow them to recover and commit into erythroid differentiation. At day four BCS was added for 72 h.

2.4. Cell lysates and immunoblots

Cells were lysed in 20 mM Hepes pH 6.8, 2 mM EDTA, 150 mM NaCl, 0.1% SDS, 0.5% Triton X-100, PMSF and HALT protease inhibitors (Thermo Scientific), centrifuged 10 min at 17,000×*g*. Supernatants were subjected to PAGE, then proteins were transferred to PVDF membranes and subjected to immunoblot detection. To detect respiratory complexes the MitoProfile total OXPHOS human antibody kit (Abcam) was used. Primary antibodies were detected with HRP-conjugated secondary antibodies and the Supersignal-Pico-West kit (Thermo Scientific).

2.5. Confocal imaging and morphometry

Cells were adhered to poly-lysine-coated coverslips, stained with 120 nM MTG for 30 min, rinsed and placed in a temperature-controlled and CO_2-supplemented chamber (Chamlide ™ IC, Live Cell Instrument, Inc) under the confocal microscope Olympus Fluoview 1000. Z-series were acquired with a slice separation of 1 μM throughout the entire cell depth. Morphometric data was extracted with Image J: number of mitochondria per cell, individual mitochondrial size and total mitochondrial area per cell.

CD34+ cell erythroid differentiation was determined by CD71-FITC (BD Pharmingen) and GPA-PE (Glycophorin A; eBioscience) staining with confocal imaging and FACS analysis.

Changes in mt$\Delta\Psi$ were determined using TMRE staining in non-quenching mode. Cells were stained for 30 min with 7 nM TMRE, single confocal images were acquired and mean fluorescence intensity per cell was quantitated using Image J. TMRE signal was also quantitated by FACS analysis.

2.6. Determination of cellular and mitochondrial ROS levels

Cells were stained with the cellular ROS marker DHE at 10 μM, or with the superoxide-sensitive dye Mitosox red, at 5 μM, for 20 min, rinsed with PBS and fluorescence intensity was detected by FACS and confocal microscopy. Intensity of Mitosox red was normalized to TMRE intensity.

2.7. FACS analysis

To detect cell death, cells were rinsed once with 10 mM Hepes, pH 7, 170 mM NaCl and incubated with 3 μL APC-Annexin V (BD Biosciences) and 30 μg/mL 7-aminoactinomycin D (7-AAD, BD Biosciences) for 15 min. To detect oxidative stress, cells were stained with 10 μM DHE or 5 μM Mitosox red (Invitrogen). Fluorescence was read using Accuri C6 cytometer (BD Biosciences) and analyzed using FCS Express (De Novo Software).

2.8. PEG-induced fusion assay

This assay was done as in Song et al., [23]. After 72 h BCS treatments, aliquots of 10^6 cells were stained with either MTG or MTR for 30 min, rinsed with PBS, mixed and allowed to fuse in the presence of 200 μL of 50% PEG for 1 min, then culture medium was added. After 6 h recovery images were acquired under epifluorescence microscope, including ~100 cells for each treatment. Mitochondrial fusion was scored visually according to the overlap of red and green signals, and classified in four categories, 0% (no fusion), <50% (most mitochondria not fused), >50% (most fused) and 100% fusion (full overlap). Results from 3 independent experiments were pooled and analyzed statistically.

2.9. Oxygen consumption rate (OCR) and extracellular acidification rate (ECAR)

Cell respiration and media acidification were measured with the XF24 (Seahorse Inc), as described in [24]. Briefly, cells were plated at 80,000 cells/well in poly-lysine-coated XF V7-PS plates and measurements were made. After obtaining basal respiration, 150 nM FCCP was added to measure maximal respiration, followed by 1 μM oligomycin. Then, 2 μM rotenone/myxothiazol were added to determine the non-mitochondrial respiration.

2.10. Statistics

Statistical analyses were performed with Graphpad Prism (Graphpad Software) with significance set at $p \leqslant 0.05$. Unpaired Student's t-test was used when comparing 2 average values. One way-ANOVA, when comparing 3 or more average values followed by Tukey's multiple comparison test, and linear regression when compared proliferation curves. Frequency distribution data from PEG-fusion assays as well as from mitochondrial confocal microscopy were analyzed through contingency tables and a chi-square test.

3. Results

3.1. Effect of copper deprivation on cellular parameters and mitochondrial morphology

To study the effects of copper deprivation on mitochondrial physiology, we used the copper chelator BCS, a hydrophilic molecule that has been widely used to chelate extracellular copper with low or no cytotoxicity in cell culture experiments [25]. We performed a BCS dose–response experiment in K562 cells to assess proliferation, apoptosis, cellular death and the ability to differentiate into erythroid cells. Proliferation decreased a 25% while apoptosis and cellular death were below 3% after 72 h. at 30 μM BCS. Although a decrease was observed in proliferation and an increase in apoptosis and cellular death, especially at higher BCS concentrations, changes in those parameters were not significantly ($p > 0.05$) different (Fig. 1A and B). However, butyrate-induced cell differentiation was significantly reduced ($p < 0.05$) in about 40% at 10 μM BCS treatment after 3 or 5 days post-induction (Fig. 1C).

Since copper deprivation was reported to generate enlarged mitochondria [11], we studied mitochondrial morphology and biomass by confocal microscopy. After image analysis and 3D reconstruction (Fig. 1 D), mitochondria from 10 μM BCS treated cells were slightly fewer and bigger (Fig. 1E and F) than control cells. Frequency distribution analysis of area of individual mitochondrial units showed, however, that the differences were significant ($p < 0.05$, chi^2 test) (Fig. 1F). Total mitochondrial area per cell was not significantly different between BCS-treated and control cells (Fig. 1G).

3.2. Expression of OXPHOS and MtDy proteins under copper deprivation

Copper deficiency is known to decrease CIV expression and activity [11,26–28]. Thus, we assessed BCS treatment effects on mitochondrial function. As seen in Fig. 2A and B, protein levels of CIV were greatly decreased (45% of control, $p \leqslant 0.05$) in BCS treated cells as compared to controls. In addition, levels of complex I and II were elevated (150% and 200% of control). No changes were detected in levels of complexes III and V.

To understand the mechanism behind the enlarged mitochondrial phenotype when under copper deprivation, we analyzed the expression of MtDy proteins as well as proteins related to mitochondrial biogenesis such as PGC-1a and porin. Interestingly, the fusion proteins MFN2 and OPA1, were significantly ($p < 0.05$) up regulated a 200% and 40% respectively, in copper-depleted cells. On the other hand, FIS1 and DRP1, the fission proteins, did not change significantly (Fig. 2C and D). Our results also showed that copper depletion does not induce mitochondrial biogenesis (Fig. 2C and D). These results are consistent with our confocal analysis.

Since MFN2 and OPA1 levels were elevated in copper-deprived cells, we next investigated whether the mitochondrial fusion rate was affected. Mitochondrial ability to fuse was assessed in PEG-induced cybrids. After 6 h post PEG-induced cytoplasmic fusion, we classified cells into 4 categories according to the extent of mitochondrial fusion (Fig. 2E). Frequency distribution analysis showed significantly ($p < 0.05$) more mitochondrial fusion in BCS-treated cells as compared to control cells (Fig. 2 F).

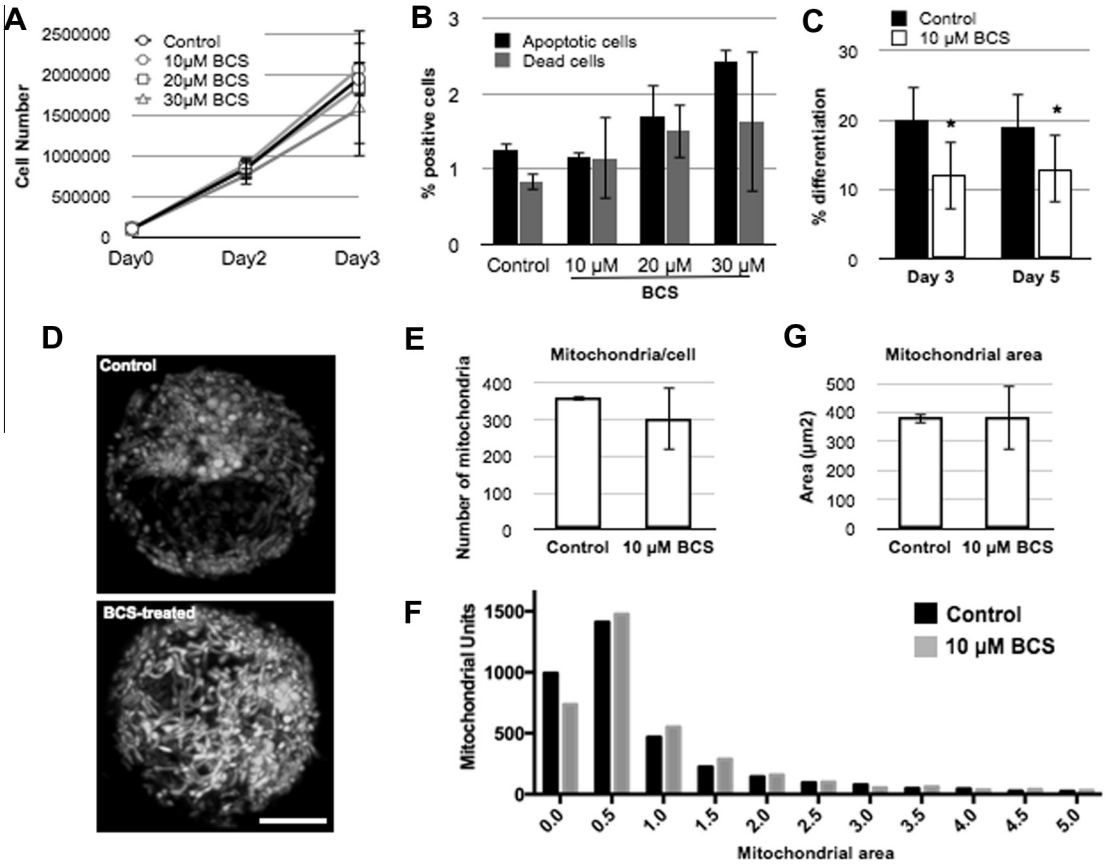

Fig. 1. Cell proliferation, differentiation and death. Mitochondrial morphology. (A) Cell proliferation in control and BCS-treated cell cultures. (B) Cell death, measured by FACS with 7-AAD and APC-Annexin V staining, in control and BCS-treated cells. Bars show % of positive-stained cells for either staining. (C) Cell differentiation. Percent of cells showing positive benzidine staining over total cell number. Control and 10 μM BCS-treated cells are shown. (D) Confocal 3D-reconstruction of mitochondrial network of control and 10 μM BCS-treated cells, stained with MTG. Bar = 5 μm. (E) Number of mitochondria per cell. (F) Individual mitochondrial area frequency distribution, in 0.5 μm^2 intervals. $n = 3$. (G) Total mitochondrial area per cell, in μm^2.

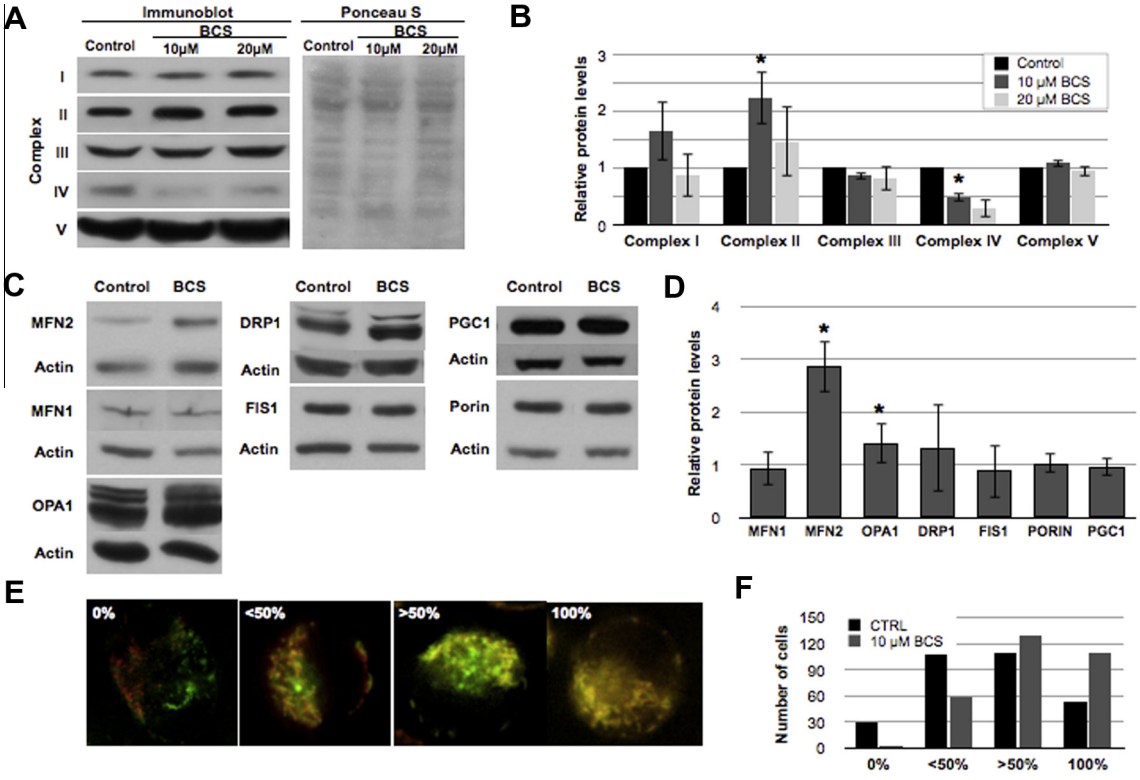

Fig. 2. Effect of copper depletion on mitochondrial proteins. (A) Immunoblots showing OXPHOS complex proteins in extracts from control or BCS-treated cells. Ponceau S-stained membrane is shown as a loading control. (B) Densitometry quantitation showing protein levels detected in copper-depleted cells, expressed as relative values over protein levels in control extracts ($n = 3$, *indicates $p \leqslant 0.05$, compared to control). (C) Immunoblot detection of mitochondrial proteins in control and 10 μM BCS-treated cells. Actin is shown as a loading control. (B) Densitometry quantitation of immunoblots. ($n = 3$, *indicates $p \leqslant 0.05$, compared to control). (E) K562 cells 6 h after PEG-induced cell fusion. Images of control single cells from each category: 0% fused mitochondria, <50% fused, >50% fused and 100% mitochondrial fusion. (F) Quantitation of mitochondrial fusion, average ± SD of the percentage of cells within each category ($n = 3$).

3.3. Bioenergetics parameters

We measured oxygen consumption, glycolysis, mtΔΨ and ROS. In BCS-treated cells, basal and maximal respiration (FCCP-stimulated) were significantly ($p < 0.05$) decreased (Fig. 3A and B) in up to 50% while basal glycolysis was significantly ($p < 0.05$) increased (Fig. 3A and B) in up to 100% in a BCS-dose response manner. This represents a metabolic switch from the mitochondrial towards the glycolytic energy-generating pathways. Maximal glycolytic rate (FCCP-stimulated) was decreased ($p < 0.05$) by BCS in a dose-dependent manner in up to 30% as compared to control cells (Fig. 3A and B). A decreased respiration allowed to build up the mtΔΨ (TMRE fluorescence) ($p < 0.05$) and to reduce the amount of ROS (Mitosox for mitochondrial ROS; DHE for total ROS) also in a BCS dependent manner ($p < 0.05$). This was observed both in confocal microscopy (Fig. 3C), FACS (Fig. 3D) and the Oxyblot technique (data not shown), which detects carbonyl groups in proteins. These results are consistent with a shut down in mitochondrial metabolism due to an inhibition of respiratory chain function in copper-depleted cells.

3.4. Copper effects on human CD34+ cells

We have described the effects of lack of copper on the erythropoietic K562 cells, a cancer cell line. To validate our results in primary cells, we exposed human CD34+ cells to BCS and measured its effect on mtΔΨ and their ability to differentiate. Interestingly, mtΔΨ significantly increased ($p < 0.05$) in a BCS-dose response manner as measured by confocal microscopy (Fig. 4A and B) and FACS (Fig. 4C). Furthermore, copper-depleted cells showed a significant ($p < 0.05$) inhibition of differentiation into the red lineage (Fig. 4D and E) given by an increase in R1 population ($p < 0.05$) and a decrease in R3 and R4 populations ($p < 0.05$). Erythroid differentiation was analyzed by the expression of the surface markers CD71 and GPA and quantified by FACS (Fig. 4D and E) where R1 represents undifferentiated cells (CD34+, CD71−, GPA−) and R4 (CD71++, GPA++), differentiated hemoglobin-containing cells. We also show representative images obtained by confocal microscopy, as well as FACS plots (Fig. 4D).

4. Discussion

Anemia and myelodysplastic syndromes are two common pathologies associated with acquired copper deprivation [6,7,10,4]. Several reports have pointed out when cells are under copper deficiency, mitochondria change their morphology toward an enlarged phenotype [11–13,29]. Moreover, the expression and activity of CIV is decreased [11,28,30–32]. Mitochondria are essential for erythropoiesis because of, besides accomplishing energy demands, they are involved in heme biosynthesis [15,16]. Thus, copper emerges as an essential cofactor, which is regulating mitochondrial morphology and function and erythropoiesis. Therefore, we wanted to study the effects of copper deprivation at the level of mitochondrial dynamics and bioenergetics in erythropoietic cells.

Initial stages of erythroid progression are characterized by an increase in mitochondrial biogenesis [33–35] and fragmentation of mitochondrial web through up-regulation of FIS1 (our unpublished results) to achieve heme biosynthesis and later on autophagy at the end of erythroid maturation [36,37]. In this regard,

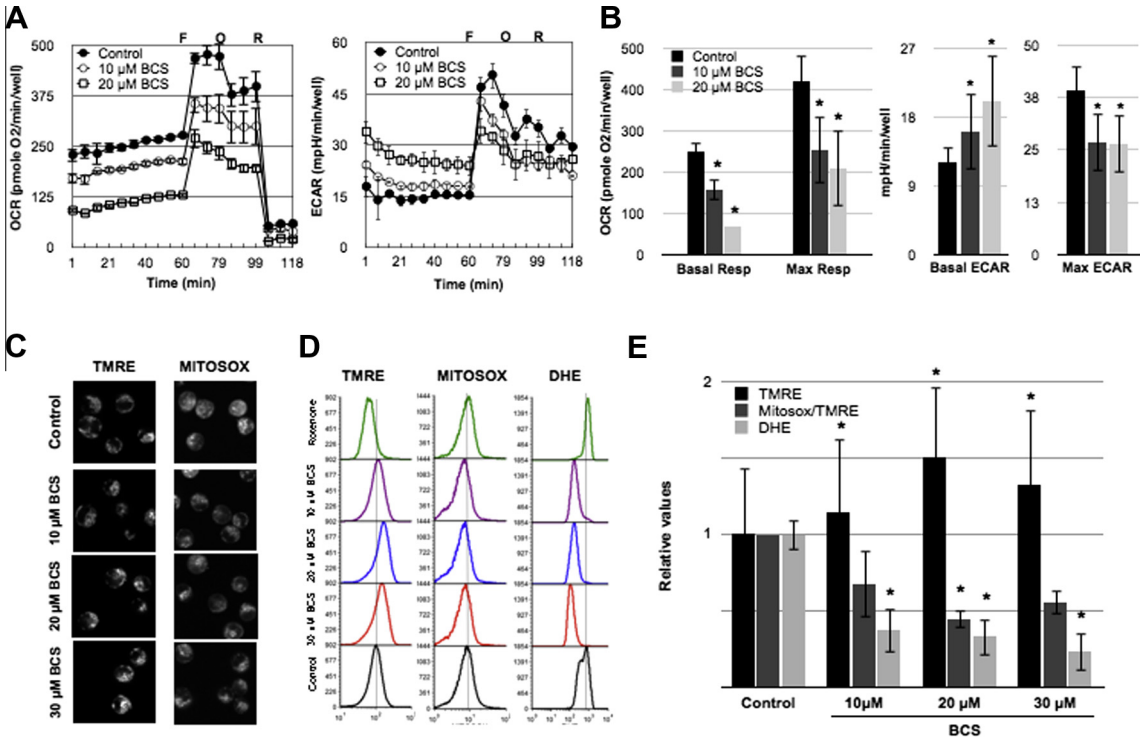

Fig. 3. Effect of copper depletion on bioenergetic parameters, membrane potential and oxidative stress. (A) OCR (left plot) and ECAR (right plot) profiles from a Seahorse XF assay. Each point is an average ± SD from 3 assay wells. Initial measurements correspond to basal respiration. At points F, O and R drugs were injected, where F: FCCP, O: oligomycin, R: rotenone. (B) OCR and ECAR average ± SD from 3 experiments. *indicates $p \leqslant 0.05$, compared to control values. (C) Images from live cells stained with TMRE (left panels) or mitosox red (right panels). One representative confocal image is shown for each treatment. (D) FACS analysis of TMRE, mitosox red and DHE-stained cells. (E) Quantitation of FACS analysis.

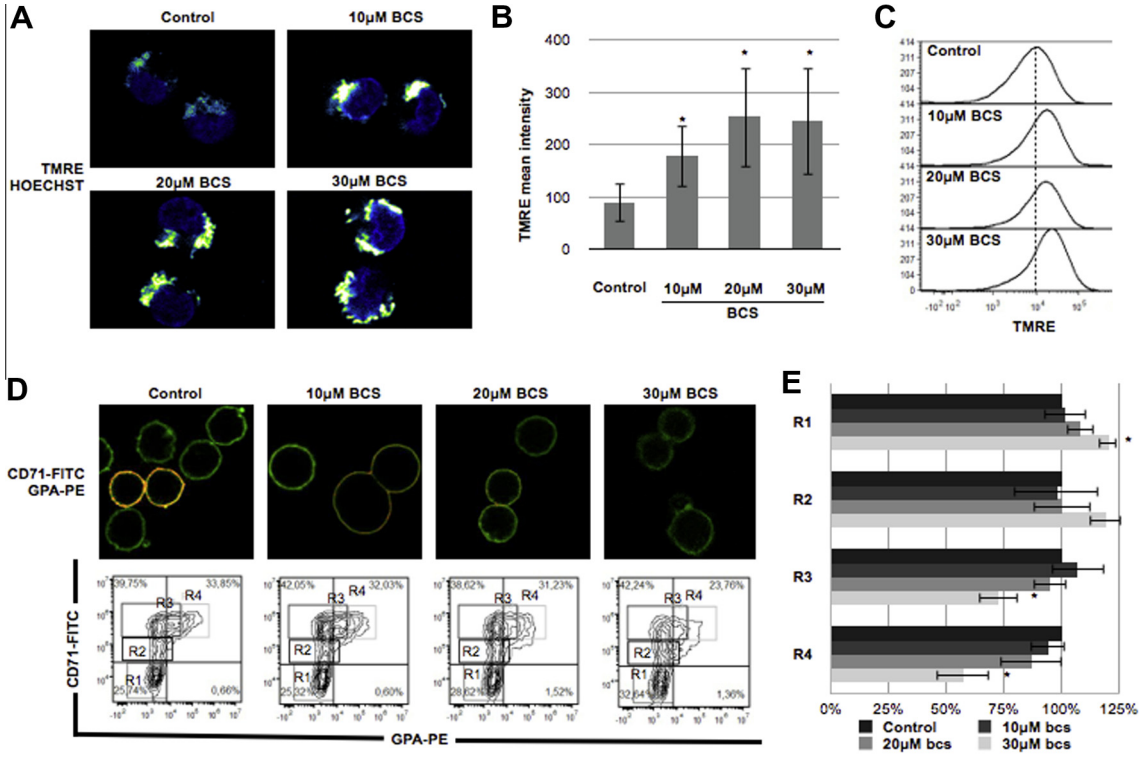

Fig. 4. Effect of copper depletion in CD34+ primary cell culture under differentiation. (A) Confocal images of control and BCS-treated CD34+ cells stained with Hoechst and TMRE shown in pseudocolor. (B) Quantitation of TMRE signal from confocal images. (C) Flow cytometry histograms of TMRE staining, one representative experiment is shown ($n = 3$). (D) CD34+ cells differentiation. Upper panels: Confocal images of control and BCS-treated cells stained with anti-CD71-FITC and anti-GPA-PE antibodies. Lower panel: Flow cytometry plots using the same antibodies, R1–R4 populations are shown, see main text. (E) Quantitation of flow cytometry experiments shown in (D). Each population was normalized to control (control = 100%). Bar graphs in (B) and (E) show average ± SD for 3 experiments. *indicates $p \leqslant 0.05$, compared to control.

formation of enlarged mitochondria when under copper deprivation could be due to an inhibition of fission events. However, our results clearly show when erythropoietic cells are copper deprived, MFN2 and OPA1 become up-regulated and functional to promote fusion. Increased fusion is thought to obey to energy requirements of the cell, availability of nutrients and health state of mitochondria [38]. Our results from mitochondrial morphology studies, even though significant, did not show the expected enlarged phenotype in copper depleted cells. In this regard, confocal microscopy may not be able to account for the real differences between normal and enlarged mitochondria, given its diffraction limit of 250 nm, which makes small organelles look bigger due to diffraction blur [39]. Copper deficiency did not alter erythropoietic cell proliferation and did not induce apoptosis in K562. Similar results were reported for HL60 cells, a white blood cell lineage [40] and hematopoietic cells [33]. However, it does impair erythroid differentiation in both K562 and CD34+ cells. Bioenergetics analysis of BCS-treated cells showed CIV levels were strongly reduced with a concomitant decrease in the basal and maximal respiration, accounting for a mitochondrial dysfunction. Given that erythropoiesis is highly dependent on mitochondrial function, our results agree with published literature on mitochondrial impairment and disruption of erythropoiesis in copper-deficient animals [33–35]. Copper deficiency-induced mitochondrial dysfunction was also associated with a loss in mt$\Delta\Psi$ in cardiac mitochondria [27] and in the C2C12 skeletal muscle cell line [28]. Interestingly, our results showed the opposite results. mt$\Delta\Psi$ was increased in a BCS dose dependent manner. Furthermore, cells showed an overall reduction in mitochondrial and cellular ROS and, in parallel, glycolysis was turned on. These results suggest that erythropoietic cells under copper deprivation make a metabolic switch from mitochondrial energy generation to glycolysis. This metabolic switch may allow them to survive while waiting for better environmental and/or nutritional conditions to move forward into differentiation. In addition, it may help to keep progenitors in an undifferentiated state [41]. It was reported that progenitor cells base most of their energy metabolism on glycolysis to avoid mitochondrial ROS production. Actually, the respiratory chain was reported not to work and mt$\Delta\Psi$ was sustained by the ATP synthase in reverse mode [42]. Beyond the basal glycolytic flux, we also show that maximal glycolytic rate is negatively affected by copper deprivation in a dose response manner. These results are supported by studies in copper-deficient mice cerebellum, which presented significantly higher concentrations of glucose and glucose-6-phosphate as compared to control animals, indicating that glycolytic metabolism is impaired [32]. Gybina et al. [32] hypothesized that higher levels of sugar might be due to an increase in NADPH/NADP+, and Rovetto et al. [43] reported inhibition of glycolysis by lactate accumulation. In our understanding, the significant low levels of ROS found in erythropoietic cells under copper deprivation, might alter the cytosolic redox environment which in turn might disrupt the NAD+ regeneration and then inhibit glycolysis.

In all, we have shown that adequate copper levels are important for maintaining proper mitochondrial function and for erythroid differentiation. Erythropoietic cells will respond to copper deprivation by turning mitochondria off, switching their metabolism toward glycolysis. The fact that mitochondria are able to adjust their own metabolism, including the up-regulation of MFN2 and OPA1 to keep the cell alive is what we have called mitochondrial adaptive responses and we believe it opens a new field in the understanding of mitochondrial physiology.

Acknowledgments

This work was funded by Postdoctorado-Fondecyt-3110171 (LR); COCHILCO-FONDECYT-1100995 (AE) and 1121078 (FS); DI-10-10R (AE); Proyecto-Núcleo-UNAB-DI-209-12/N (AE; FS; CR). Millennium Institute on Immunology and Immunotherapy P09-016-F . We also thank the Maternity Service at Complejo Asistencial Barros Luco for its participation in this study.

References

[1] B.-E. Kim, T. Nevitt, D.J. Thiele, Mechanisms for copper acquisition, distribution and regulation, Nat. Chem. Biol. 4 (2008) 176–185.
[2] D. Horn, A. Barrientos, Mitochondrial copper metabolism and delivery to cytochrome c oxidase, IUBMB Life 60 (2008) 421–429.
[3] M.L. Turski, D.J. Thiele, New roles for copper metabolism in cell proliferation, signaling, and disease, J. Biol. Chem. (2009).
[4] M.S. Willis, S.A. Monaghan, M.L. Miller, R.W. McKenna, W.D. Perkins, B.S. Levinson, et al., Zinc-induced copper deficiency, Am. J. Clin. Pathol. 123 (2004) 125–131.
[5] K. Doherty, M. Connor, R. Cruickshank, Zinc-containing denture adhesive: a potential source of excess zinc resulting in copper deficiency myelopathy, Br. Dent. J. 210 (2011) 523–525.
[6] D.P. Griffith, D.A. Liff, T.R. Ziegler, G.J. Esper, E.F. Winton, Acquired copper deficiency: a potentially serious and preventable complication following gastric bypass surgery, Obesity 17 (2012) 827–831.
[7] N. Jabbour, J.A. DiGiuseppe, S. Usmani, S. Tannenbaum, Copper deficiency as a cause of reversible anemia and neutropenia, Conn. Med. 74 (2010) 261–263.
[8] S.R. Jaiser, G.P. Winston, Copper deficiency myelopathy, J. Neurol. 257 (2010) 869–881.
[9] L. Bolamperti, M.A. Leone, A. Stecco, M. Reggiani, M. Pirisi, A. Carriero, et al., Myeloneuropathy due to copper deficiency: clinical and MRI findings after copper supplementation, Neurol. Sci. 30 (2009) 521–524.
[10] T. Fong, R. Vij, A. Vijayan, J. DiPersio, M. Blinder, Copper deficiency: an important consideration in the differential diagnosis of myelodysplastic syndrome, Haematologica 92 (2007) 1429–1430.
[11] P.R. Dallman, J.R. Goodman, Enlargement of mitochondrial compartment in iron and copper deficiency, Blood 35 (1970) 496–505.
[12] C.H. Gallagher, V.E. Reeve, R. Wright, Cooper deficiency in the rat effect on the ultrastructure of hepatocytes, Immunol. Cell Biol. 51 (1973) 181–189.
[13] J.R. Goodman, J.B. Warshaw, P.R. Dallman, Cardiac hypertrophy in rats with iron and copper deficiency: quantitative contribution of mitochondrial enlargement, Pediatr. Res. 4 (1970) 244–256.
[14] T. Wakabayashi, M. Asano, C. Kurono, Mechanism of the formation of megamitochondria induced by copper-chelating agents Z, Pathol. Int. 25 (1975) 15–37.
[15] J. Chung, C. Chen, B.H. Paw, Heme metabolism and erythropoiesis, Curr. Opin. Hematol. 19 (2012) 156–162.
[16] M. Fontenay, S. Cathelin, M. Amiot, E. Gyan, E. Solary, Mitochondria in hematopoiesis and hematological diseases, Oncogene 25 (2006) 4757–4767.
[17] X. An, N. Mohandas, Erythroblastic islands, terminal erythroid differentiation and reticulocyte maturation, Int. J. Hematol. 93 (2011) 139–143.
[18] M.S. Carraway, H.B. Suliman, W.S. Jones, C.-W. Chen, A. Babiker, C.A. Piantadosi, Erythropoietin activates mitochondrial biogenesis and couples red cell mass to mitochondrial mass in the heart, Circ. Res. 106 (2010) 1722–1730.
[19] J. Zhao, U. Lendahl, M. Nistér, Regulation of mitochondrial dynamics: convergences and divergences between yeast and vertebrates, Cell. Mol. Life Sci. 70 (2013) 951–976.
[20] Y. Yoon, E.W. Krueger, B.J. Oswald, M.A. McNiven, The mitochondrial protein hFis1 regulates mitochondrial fission in mammalian cells through an interaction with the dynamin-like protein DLP1, Mol. Cell. Biol. 23 (2003) 5409–5420.
[21] C.-R. Chang, C. Blackstone, Dynamic regulation of mitochondrial fission through modification of the dynamin-related protein Drp1, Ann. NY Acad. Sci. 1201 (2010) 34–39.
[22] M.-C. Giarratana, L. Kobari, H. Lapillonne, D. Chalmers, L. Kiger, T. Cynober, et al., Ex vivo generation of fully mature human red blood cells from hematopoietic stem cells, Nat. Biotechnol. 23 (2005) 69–74.
[23] Z. Song, M. Ghochani, J.M. McCaffery, T.G. Frey, D.C. Chan, Mitofusins and OPA1 mediate sequential steps in mitochondrial membrane fusion, Mol. Biol. Cell 20 (2009) 3525–3532.
[24] M. Wu, A. Neilson, A.L. Swift, R. Moran, J. Tamagnine, D. Parslow, et al., Multiparameter metabolic analysis reveals a close link between attenuated mitochondrial bioenergetic function and enhanced glycolysis dependency in human tumor cells, Am. J. Physiol. Cell Physiol. 292 (2007) C125–C136.
[25] X. Ding, H. Xie, Y.J. Kang, The significance of copper chelators in clinical and experimental application, J. Nutr. Biochem. 22 (2011) 301–310.
[26] D.M. Medeiros, R.E. Wildman, Newer findings on a unified perspective of copper restriction and cardiomyopathy, Proc. Soc. Exp. Biol. Med. 215 (1997) 299–313.
[27] X. Chen, D.B. Jennings, D.M. Medeiros, Impaired cardiac mitochondrial membrane potential and respiration in copper-deficient rats, J. Bioenerg. Biomembr. 34 (2002) 397–406.
[28] X. Chen, D.M. Medeiros, D. Jennings, Mitochondrial membrane potential is reduced in copper-deficient C2C12 cells in the absence of apoptosis, Biol. Trace Elem. Res. 106 (2005) 51–64.

[29] T. Wakabayashi, Megamitochondria formation – physiology and pathology, J. Cell Mol. Med. 6 (2002) 497–538.
[30] D.M. Medeiros, L. Shiry, T. Samelman, Cardiac nuclear encoded cytochrome c oxidase subunits are decreased with copper restriction but not iron restriction: gene expression, protein synthesis and heat shock protein aspects, Comp. Biochem. Physiol. A Physiol. 117 (1997) 77–87.
[31] H. Zeng, J.T. Saari, W.T. Johnson, Copper deficiency decreases complex IV but not complex I, II, III, or V in the mitochondrial respiratory chain in rat heart, J. Nutr. 137 (2007) 14–18.
[32] A.A. Gybina, J.R. Prohaska, Fructose-2,6-bisphosphate is lower in copper deficient rat cerebellum despite higher content of phosphorylated amp-activated protein kinase, Exp. Biol. Med. 233 (2008) 1262–1270.
[33] S.-I. Inoue, S. Noda, K. Kashima, K. Nakada, J.-I. Hayashi, H. Miyoshi, Mitochondrial respiration defects modulate differentiation but not proliferation of hematopoietic stem and progenitor cells, FEBS Lett. 584 (2010) 3402–3409.
[34] S.-I. Inoue, M. Yokota, K. Nakada, H. Miyoshi, J.-I. Hayashi, Pathogenic mitochondrial DNA-induced respiration defects in hematopoietic cells result in anemia by suppressing erythroid differentiation, FEBS Lett. 581 (2007) 1910–1916.
[35] V.G. Sankaran, S.H. Orkin, C.R. Walkley, Rb intrinsically promotes erythropoiesis by coupling cell cycle exit with mitochondrial biogenesis, Sci. Signal. (2008).
[36] M. Chen, H. Sandoval, J. Wang, Selective mitochondrial autophagy during erythroid maturation, Autophagy 4 (2008) 926–928.
[37] H. Sandoval, P. Thiagarajan, S.K. Dasgupta, A. Schumacher, J.T. Prchal, M. Chen, et al., Essential role for Nix in autophagic maturation of erythroid cells, Nature 454 (2008) 232–235.
[38] A. Santel, Get the balance right: mitofusins roles in health and disease, Biochim. Biophys. Acta 1763 (2006) 490–499.
[39] A. Kaasik, D. Safiulina, A. Zharkovsky, V. Veksler, Regulation of mitochondrial matrix volume, Am. J. Physiol 292 (2007) C157–C163.
[40] S.S.S. Percival, M.M. Layden-Patrice, HL-60 cells can be made copper deficient by incubating with tetraethylenepentamine, J. Nutr. 122 (1992) 2424–2429.
[41] T. Peled, E. Glukhman, N. Hasson, S. Adi, H. Assor, D. Yudin, et al., Chelatable cellular copper modulates differentiation and self-renewal of cord blood-derived hematopoietic progenitor cells, Exp. Hematol. 33 (2005) 1092–1100.
[42] J. Zhang, I. Khvorostov, J.S. Hong, Y. Oktay, L. Vergnes, E. Nuebel, et al., UCP2 regulates energy metabolism and differentiation potential of human pluripotent stem cells, EMBO J. 30 (2011) 4860–4873.
[43] M.J. Rovetto, W.F. Lamberton, J.R. Neely, Mechanisms of glycolytic inhibition in ischemic rat hearts, Circ. Res. 37 (1975) 742–751.